chemosensors

MDPI

Article

MOF-Based Materials with Sensing Potential: Pyrrolidine-Fused Chlorin at UiO-66(Hf) for Enhanced NO_2 Detection

Carla Queirós [1], Francisco G. Moscoso [2], José Almeida [1], Ana M. G. Silva [1], Ahmad Sousaraei [3], Juan Cabanillas-González [3], Manuela Ribeiro Carrott [4], Tânia Lopes-Costa [2], José M. Pedrosa [2,*] and Luís Cunha-Silva [1,*]

[1] LAQV-REQUIMTE, Department of Chemistry and Biochemistry, Faculty of Sciences, University of Porto, 4169-007 Porto, Portugal; carla.queiros@fc.up.pt (C.Q.); j.almeida@fc.up.pt (J.A.); ana.silva@fc.up.pt (A.M.G.S.)
[2] Department of Physical, Chemical and Natural Systems, University Pablo de Olavide, Ctra. Utrera Km. 1, 41013 Sevilla, Spain; fgarciamoscoso@gmail.com (F.G.M.); tlopcos@upo.es (T.L.-C.)
[3] Madrid Institute for Advanced Studies in Nanoscience, IMDEA Nanociencia, Calle Faraday 9, Universitaria de Cantoblanco, 28049 Madrid, Spain; ahmad.sousaraei@imdea.org (A.S.); juan.cabanillas@imdea.org (J.C.-G.)
[4] LAQV-REQUIMTE, Institute for Research and Advanced Studies, Department of Chemistry and Biochemistry, School of Sciences and Technology, University of Évora, 7000-671 Évora, Portugal; manrc@uevora.pt
* Correspondence: jmpedpoy@upo.es (J.M.P.); l.cunha.silva@fc.up.pt (L.C.-S.)

Citation: Queirós, C.; Moscoso, F.G.; Almeida, J.; Silva, A.M.G.; Sousaraei, A.; Cabanillas-González, J.; Ribeiro Carrott, M.; Lopes-Costa, T.; Pedrosa, J.M.; Cunha-Silva, L. MOF-Based Materials with Sensing Potential: Pyrrolidine-Fused Chlorin at UiO-66(Hf) for Enhanced NO_2 Detection. *Chemosensors* **2022**, *10*, 511. https://doi.org/10.3390/chemosensors10120511

Academic Editors: Yonghai Song and Fugang Xu

Received: 3 November 2022
Accepted: 29 November 2022
Published: date

Table of Contents

1. TCPC and TCPP Amount Determination in the MOFs

The amount of TCPC and TCPP in the MOFs prepared by one-pot solvothermal reaction (TCPC@MOF and TCPP@MOF) was determined using a standard curve reported method [1] In summary, TCPC and TCPP standard solutions were prepared in a 1:1 mixture of NaOH (2 M) aqueous solution/DMF and linear fitting of the absorbance at 419 nm was plotted. The MOFs were digested in the same solvents mixture until no more powder was observed (clear solution), UV-Vis spectra were obtained and used to determine the amount of TCPC and TCPP in the MOFs.

2. Scanning Electron Microscopy (SEM) and Energy-Dispersive X-Ray Spectroscopy (EDS)

2.1. SEM of TCPC, TCPP, TCPC@MOF and TCPP@MOF

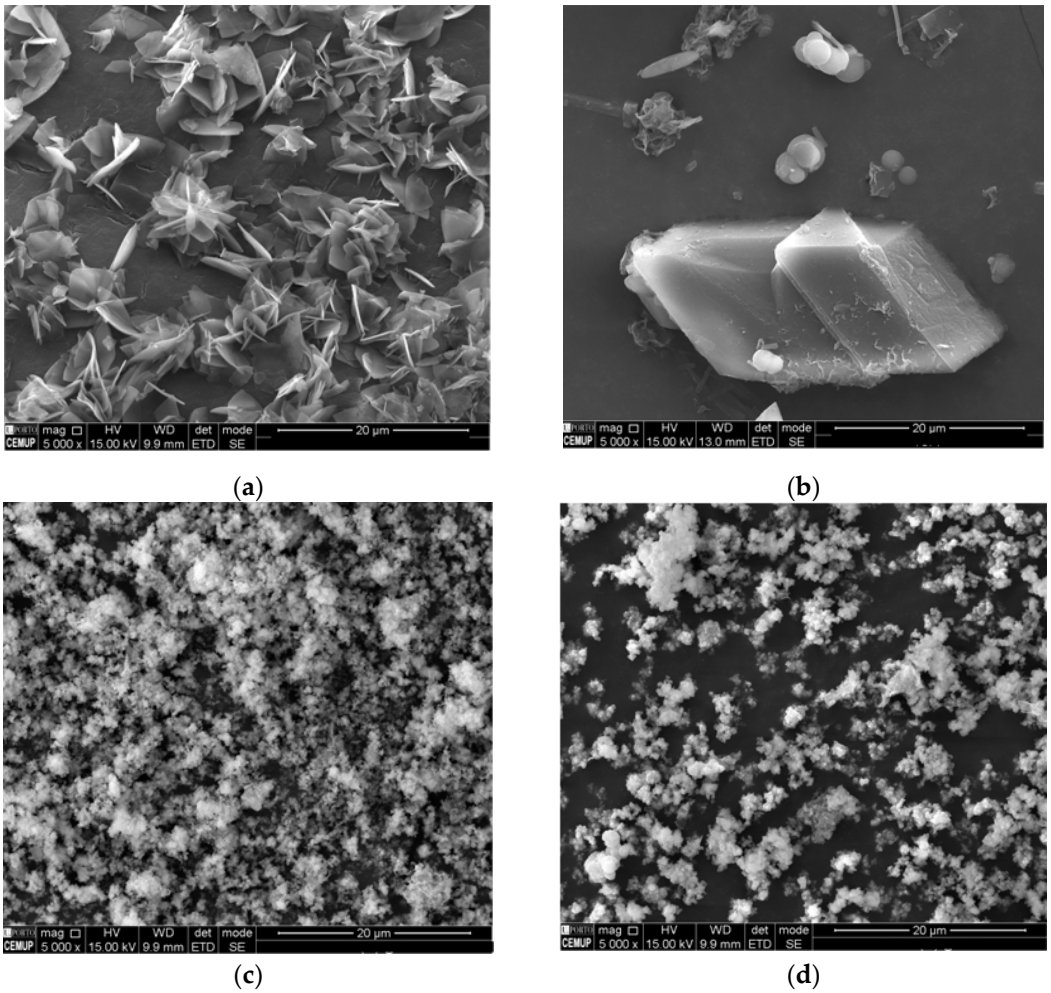

(**a**) (**b**)

(**c**) (**d**)

Figure S1. Scanning electron microscopy (SEM) images of TCPC (**a**), TCPP (**b**), TCPC@MOF (**c**) and TCPP@MOF (**d**).

2.2. EDS of TCPC, TCPP, UIO-66(HF), TCPC@MOF and TCPP@MOF

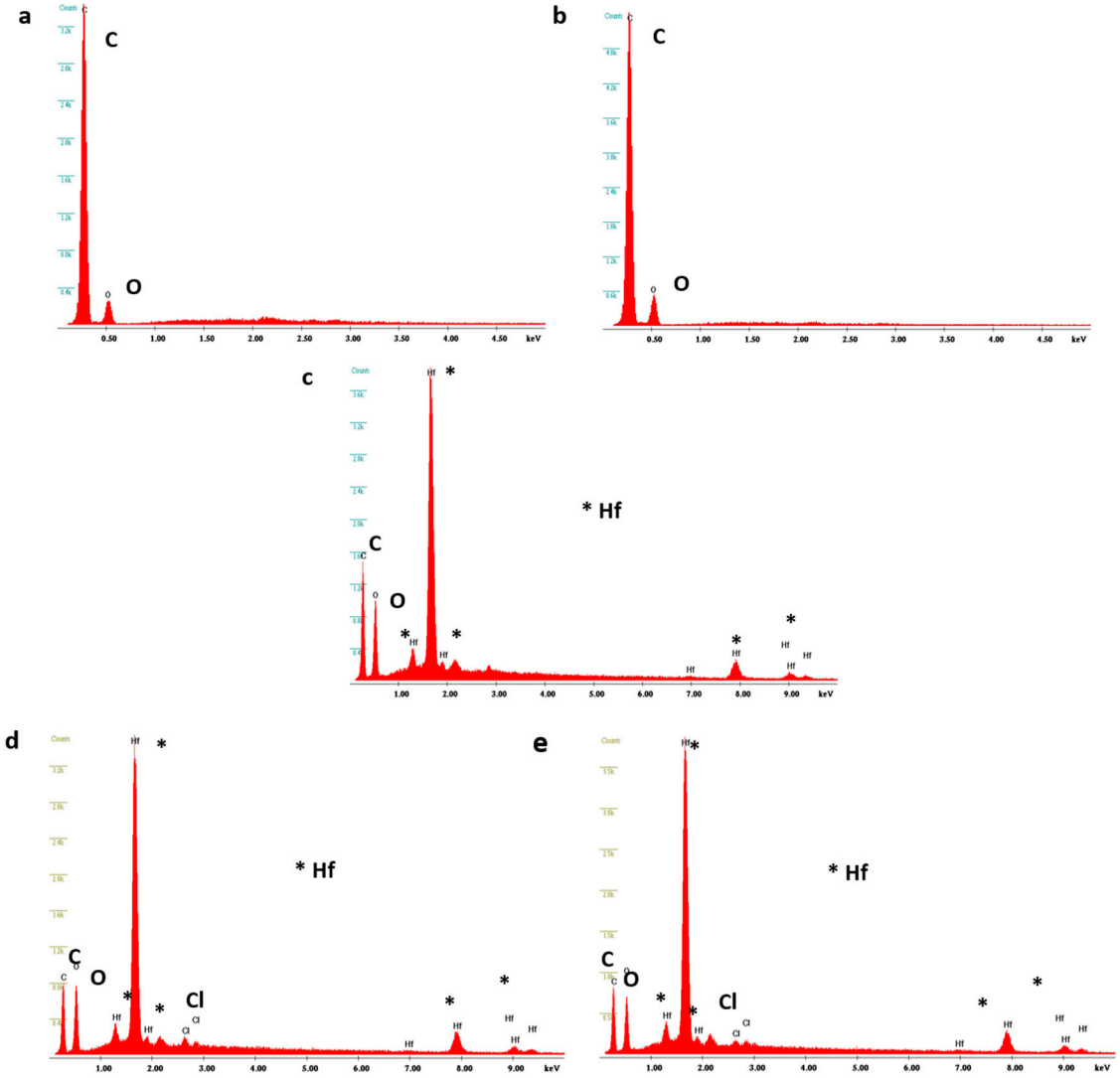

Figure S2. EDS graphical representations of TCPC (**a**), TCPP (**b**), UiO-66(Hf) (**c**), TCPC@MOF (**d**) and TCPP@MOF (**e**).

3. Fourier-Transform Infrared Spectroscopy (FTIR)

3.1. FTIR of TCPC, TCPP, UiO-66(Hf), TCPC@MOF and TCPP@MOF

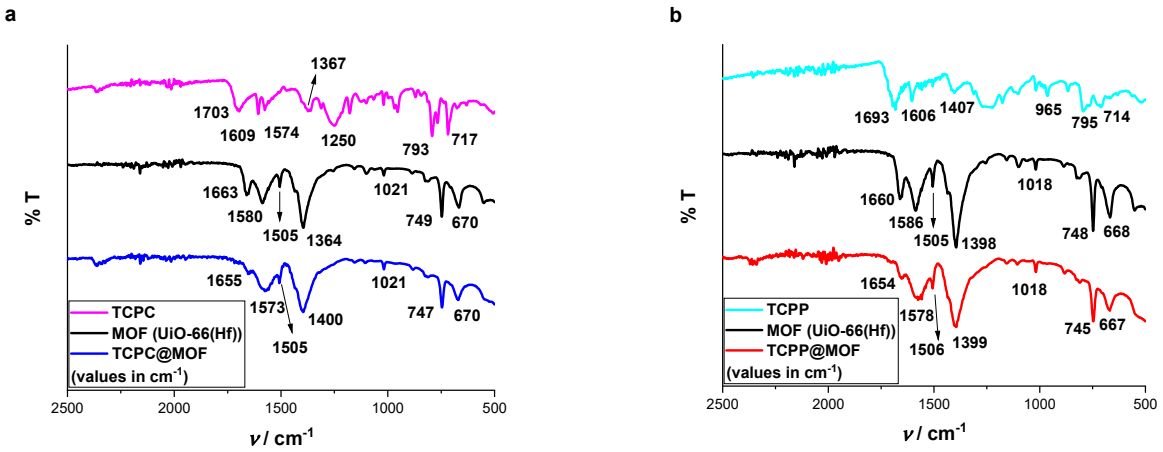

(**a**) (**b**)

Figure S3. FTIR-ATR spectra of (**a**): TCPC, MOF (UiO-66(Hf)) and TCPC@MOF and (**b**): TCPP, MOF (UiO-66(Hf)) and TCPP@MOF in the range 2500–500 cm^{-1}.

4. Zeta Potential (ζ)

4.1. Zeta Potential of TCPC, TCPP and MOFs in Milli-Q Water and Ethanol

Table S1. Zeta potential (ζ) values for TCPC, TCPP and MOFs (UiO-66(Hf), TCPC@MOF and TCPP@MOF) in milli-Q water/ethanol at 25 °C.

	ζ (mV)	
Derivative/MOF	**Milli-Q water**	**Ethanol**
TCPC	−28.1 ± 0.6	
TCPP	−33.5 ± 0.8	
UiO-66(Hf)	−3.2 ± 0.8	−23.3 ± 0.2
TCPC@MOF	−8.6 ± 0.6	−7.7 ± 0.4
TCPP@MOF	−4.7 ± 0.3	29.7 ± 0.8

5. Optical Properties

Table S2. Absorption and emission properties of TCPC, TCPP, UiO-66(Hf), TCPC@MOF, TCPP@MOF in ethanol, at 25 °C.

Compound	λ_{abs}/nm(ε/$M^{-1}cm^{-1}$)	λ_{em}/nm
TCPC	419 (6.84 × 10^5), 514 (8.76 × 10^4), 542 (5.42 × 10^4), 595 (2.52 × 10^4), 648 (1.14 × 10^5)	650, 715
TCPP	416 (2.24 × 10^5), 513 (1.39 × 10^4), 548 (8.72 × 10^3), 590 (5.86 × 10^3), 646 (4.55 × 10^3)	649, 716
UiO-66(Hf)	266	
TCPC@MOF	441, 531, 564, 609, 660	656, 719
TCPP@MOF	438, 530, 562, 607, 660	658, 719

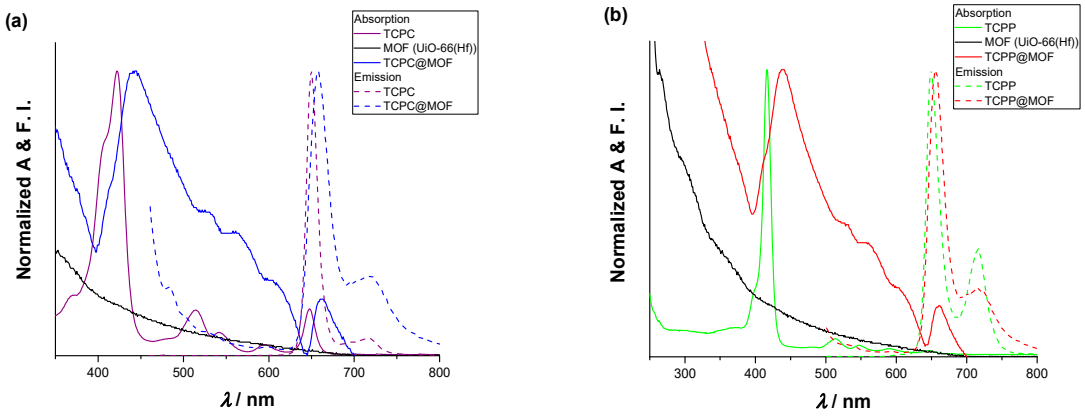

(**a**) (**b**)

Figure S4. Normalized absorption and emission spectra in ethanol (25 °C) of: (**a**) TCPC (violet solid and dashed lines), MOF (UiO-66(Hf), black line) and TCPC@MOF (blue solid and dashed lines) and (**b**) TCPP (green solid and dashed lines), MOF (UiO-66(Hf), black line) and TCPP@MOF (red solid and dashed lines).

6. Thermogravimetry Analysis (TGA)

6.1. TGA of TCPC and TCPP

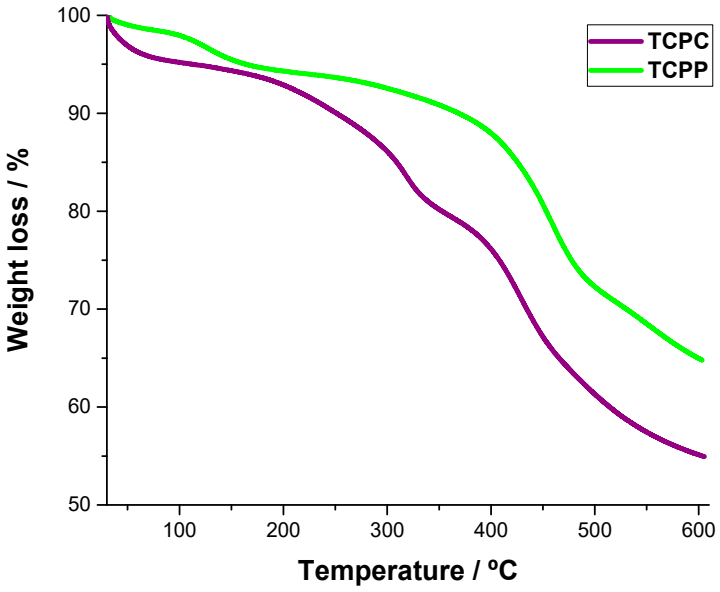

Figure S5. TGA of TCPC (purple line) and TCPP (green line) from 30 to 600 °C performed with a heating rate of 5 °C/min in a 200 cm^3/min N_2 flow stream.

7. Time-Resolved Photoluminescence Decay Curves

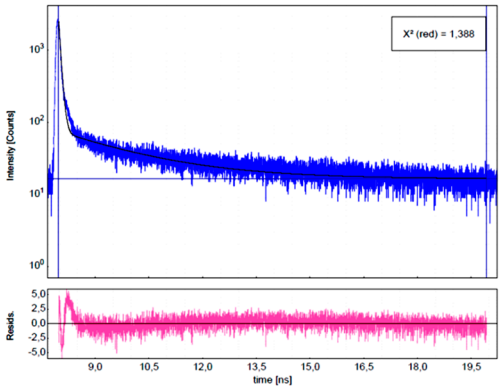

(**a**)

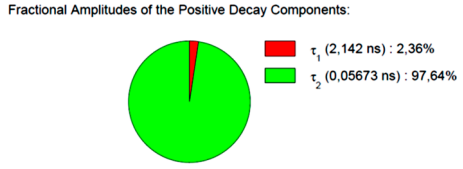

(**b**)

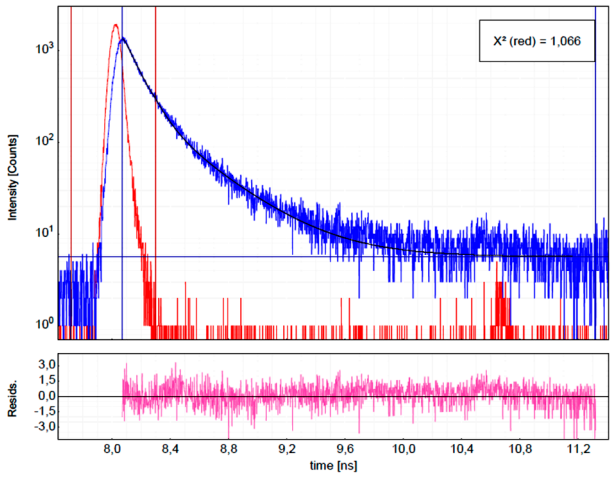

(**c**)

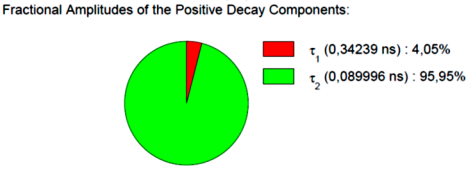

(**d**)

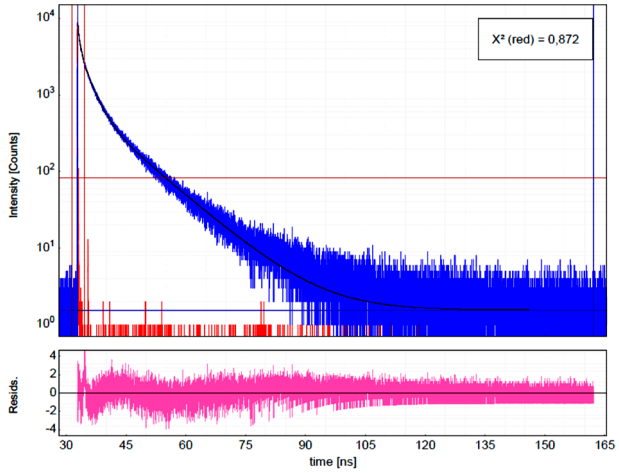

(**e**)

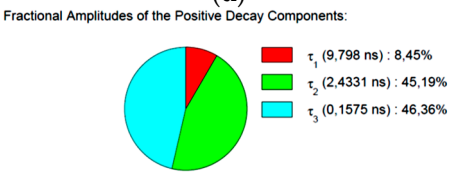

(**f**)

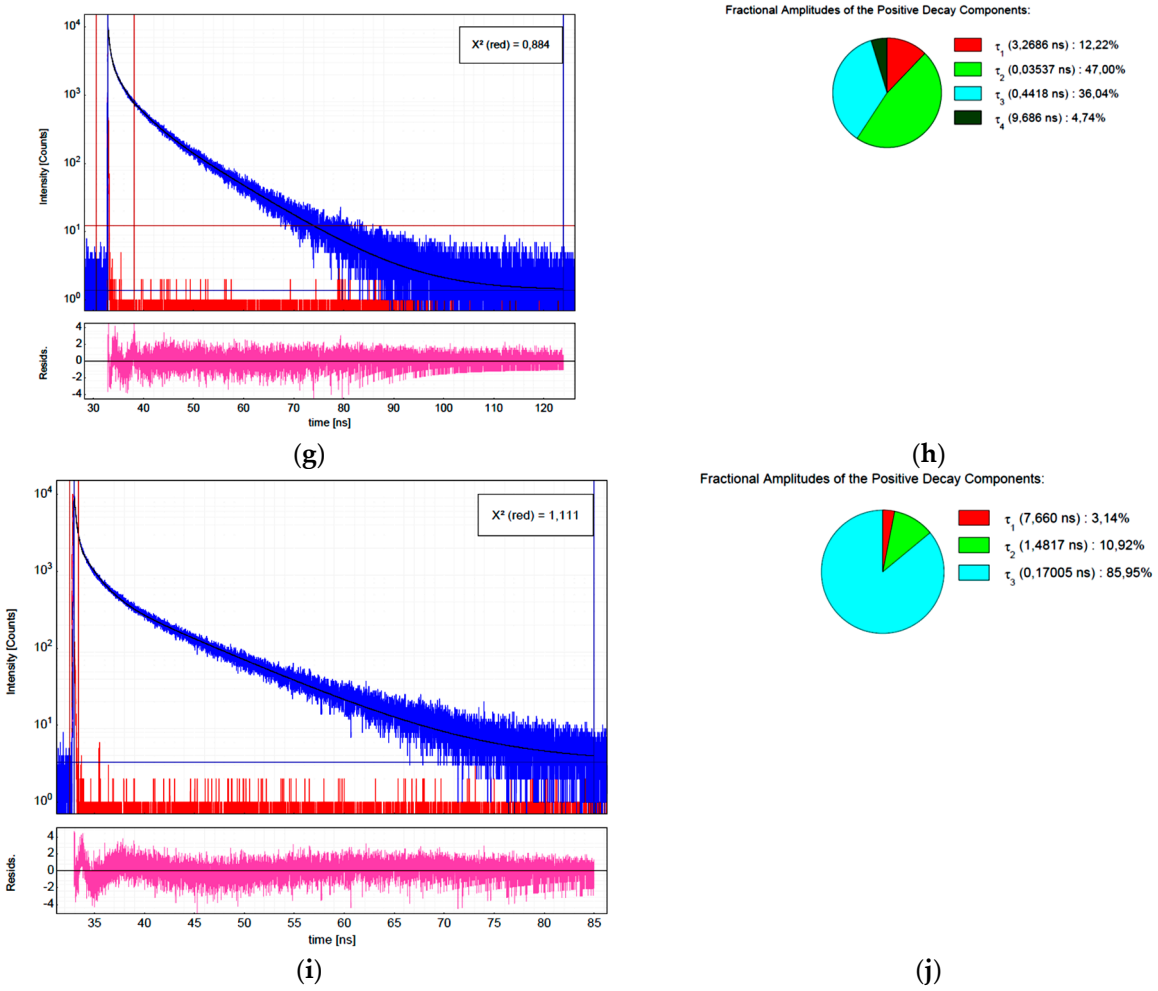

Figure S6. PL decay curves (blue) of the different samples. (**a**–**b**): PL decay of TCPC; (**c**–**d**): PL decay of TCPP; (**e**–**f**): PL decay of UiO66(Hf); (**g**–**h**): PL decay of TCPC@MOF; (**i**–**j**): PL decay of TCPP@MOF. Multi-exponential fits are shown as black lines with the individual decay components and fractional amplitudes displayed on the right. The red lines stand for the instrumental response function which was employed deconvoluted from each PL decay trace.

8. Emission Spectra of PDMS Films Prepared with the MOFs

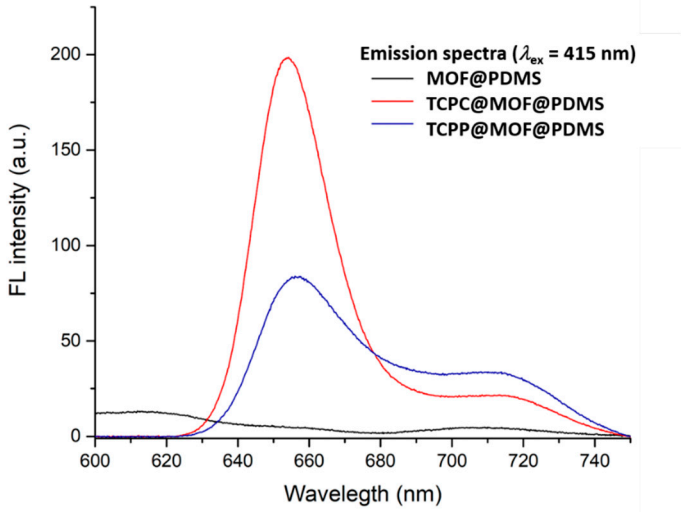

Figure S7. Comparison of PL emission spectra between MOF@PDMS (black line), TCPC@MOF@PDMS (red line) and TCPP@MOF@PDMS (blue line) films.

9. Emission Spectra of TCPC@MOF@PDMS

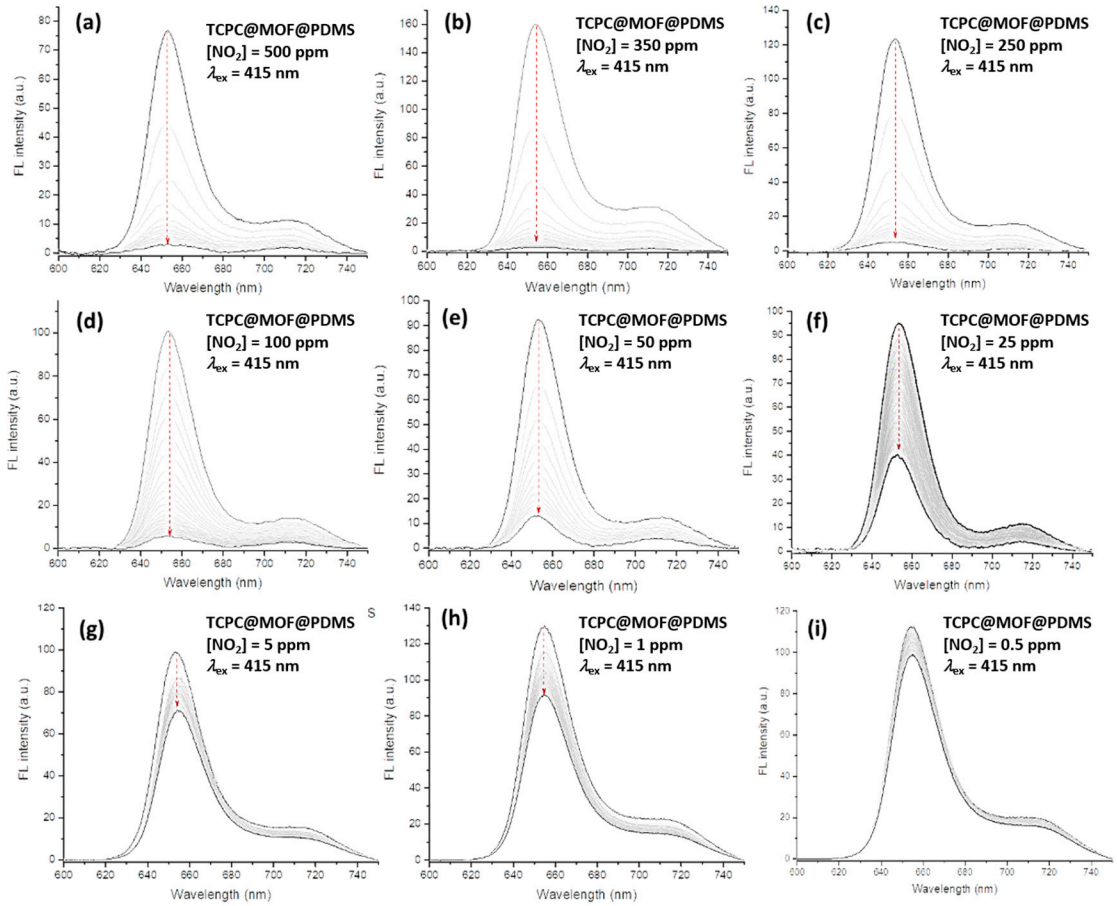

Figure S8. Time evolution (interval 5 min) of the PL emission spectra of TCPC@MOF@PDMS at different concentrations of NO_2 gas.

References

1. Ni, M.; Gong, M.; Li, X.; Gu, J.; Li, B.; Chen, Y. Dimensions of fluorescence kinetic concentration of doped morphology homologs synthesized by TCPP and UiO-66 MOF. *Appl. Mater. Today* **2021**, *23*, 100982.